Available online at www.sciencedirect.com
SCIENCE DIRECT®
Journal of Nuclear Materials 336 (2005) 54–64
journal of nuclear materials
www.elsevier.com/locate/jnucmat

Hydride phase dissolution enthalpy in neutron irradiated Zircaloy-4

P. Vizcaíno, A.D. Banchik *, J.P. Abriata

Centro Atómico Ezeiza, Centro atómico Bariloche, Comisión Nacional de Energía Atómica, Av. Del Libertador 8250, CP 1429, Buenos Aires, Argentina

Received 4 January 2004; accepted 31 August 2004

Abstract

The differential calorimetric technique has been applied to measure the dissolution enthalpy, $\Delta H^{\text{irrad}}_{\delta\to\alpha}$, of zirconium hydrides precipitated in structural components removed from the Argentine Atucha 1 PHWR nuclear power plant after 10.3 EFPY. An average value of $\Delta H^{\text{irrad}}_{\delta\to\alpha} = 5$ kJ/mol H was obtained after the first calorimetric run. That value is seven times lower than the value of $\Delta H_{\delta\to\alpha} = 37.7$ kJ/mol H recently determined in Zircaloy-4 specimens taken from similar unirradiated structural components using the same calorimetric technique [P. Vizcaíno, PhD thesis, Number TD-11/03, Inst. Tech. 'Prof. Jorge A. Sábato', CICAC, CNEA, Buenos Aires, Argentina, 24 June 2003]. Post-irradiation thermal treatments gradually increase that low value towards the unirradiated value with increasing annealing temperature similar to that observed for $\text{TSSd}_{\text{irrad}}$ [P. Vizcaíno, A.D. Banchik, J.P. Abriata. J. Nucl. Mater. 304/2–3 (2002) 96–106]. Therefore the same H atom trapping mechanism during reactor operation already proposed to explain the evolution of $\text{TSSd}_{\text{irrad}}$ is also valid for $Q^{\text{irrad}}_{\delta\to\alpha}$. As the ratio $Q/\Delta H$ is proportional to the number N_{H} of H atoms precipitated as hydrides, the increment of $Q^{\text{irrad}}_{\delta\to\alpha}$ with the thermal treatment indicates that the value of N_{H} also grows with the annealing reaching the value corresponding to the bulk H concentration when $\Delta H^{\text{irrad}}_{\delta\to\alpha} \approx 37$ kJ/mol H. That is a direct indication that the post-irradiation thermal treatment releases the H atoms from their traps increasing the number of H atoms available to precipitate at the end of each calorimetric run and/or isothermal treatment.

1. Introduction

The thermodynamic properties of the solvus of the Zr–H system have been thoroughly studied. Two reviews were made in the '90s where the great amount of information available was analyzed, selecting the best data for the building of a phase diagram and putting special emphasis on the *solvus* thermodynamic properties [3,4]. It is well known that the neutron irradiation environment in the nuclear core dramatically modifies the original properties of the materials. Even though the hydrides are involved in relevant cracking mechanisms of Zr-base structural components, only one paper was found on the effect of neutron irradiation on Zr–H system [5]. Thus, a post-irradiation research program has been implemented in our laboratory, focusing on the study of the hydrogen solubility in Zircaloy-4. In the first study, the terminal solid solubility during hydride dissolution, $\text{TSSd}_{\text{irrad}}$, was

* Corresponding author.
E-mail address: banchik@cae.cnea.gov.ar (A.D. Banchik).

0022-3115/$ - see front matter © 2004 Elsevier B.V. All rights reserved.
doi:10.1016/j.jnucmat.2004.08.013

measured with a differential scanning calorimeter (DSC) [2]. The material was taken from two Zircaloy-4 cooling channels removed from the Atucha 1 PHWR nuclear power station (CNA1) located in Argentina. These channels operated at full power for 10.3 years, reaching a neutron fluence of about 10^{22} n/cm^2 in the areas subject to the greatest neutron flux. The most relevant result of this work is an important increase of the hydrogen solubility in the two-phase field. However that is a metastable effect because post-irradiation thermal treatments gradually increase $TSSd_{irrad}$ toward the unirradiated value. A trapping mechanism of H atoms by irradiation induced defects was proposed to explain the results. That model could explain both the low value of $TSSd_{irrad}$ because only a fraction of the H concentration is free to precipitate as hydrides, and the reversion of the solubility increment because the thermal treatment release the H atoms from the traps possibly because the annealing dissolves the irradiation defects. However there are other potential explanations. A metastable intermediate hydride of low enthalpy formation could be an alternative possibility.

No determinations of solvus enthalpy in irradiated material have been made yet. The enthalpy controls the hydride phase dissolution; consequently, it would help to interpret the results obtained in $TSSd_{irrad}$ because the solvus enthalpy is just proportional to the amount of H atoms precipitated as hydrides.

The enthalpy has been obtained by measuring the dissolution heat, $Q^{irrad}_{\delta\to\alpha}$, directly, using a differential scanning calorimeter already described [2]. To determinate the effect of irradiation and simplify the interpretation, TSSd and the dissolution heat $Q_{\delta\to\alpha}$ were measured in unirradiated Zircaloy-4 hydrided at the laboratory with a microstructure similar to that of the irradiated material.

The results obtained in the irradiated material strengthen the hypothesis on hydrogen traps in irradiation-generated defects presented in a previous work [2].

The present work is organized in the following way: Section 2 describes the criteria used to measure TSSd, $Q_{\delta\to\alpha}$ and the treatment given to the calorimetric curve in order to correct the base line slope. Section 3 describes irradiated and unirradiated material, a detail of the procedure followed to add hydrogen to unirradiated material and the DSC experiment scheduling for both materials. Section 4 presents the results obtained for irradiated and unirradiated material and, finally, Sections 5 and 6 respectively present the discussion and conclusions.

2. Experimental

2.1. Calorimetry

The instrument used for TSSd and $Q_{\delta\to\alpha}$ measurements is the model DSC-60 by Shimadzu, which has already been described [2].

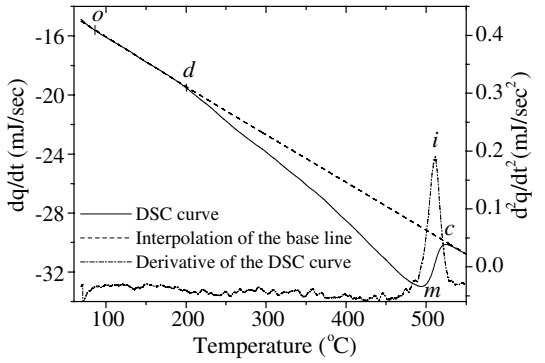

Fig. 1. DSC curve from a hydrided Zircaloy-4 sample (480 ppm-H), with no reference sample.

In differential calorimetry, the *base line* is the curve obtained in a calorimetric run with empty crucibles. The base line is usually horizontal. If a run is performed with a Zircaloy-4 hydrided sample, a curve similar to that of Fig. 1 is obtained. The DSC detects the start of the transformation between 150 and 160 °C (point *d*, temperature T_d); at this temperature the solubility in α phase is 4–5 hydrogen ppm. At this point, the curve deviates from the base line until the dissolution ends. When this happens, a slope change at point *m* (minimum, temperature T_m) occurs, then a new slope change occurs at the inflection point *i* (temperature T_i) and finally the curve returns to the original base line at completion point *c* (temperature T_c). In a sample with a concentration that is close to the αZr phase solubility limit (about 650 ppm) the dissolution process extends to 550 °C. In said curve, points *c* and *d* will be separated by a 400 °C interval. In such a wide temperature range, the base line is not horizontal mainly because of constructive asymmetries in the DSC crucibles and furnace. If this slope is significant, a systematic error will be introduced in the TSSd measurement.

Then, the heat per unit of time $dq(t)/dt$ vs time curve is calculated subtracting from the calorimetric experimental curve an interpolation curve drawing between points *d* and *c* (Fig. 1). Usually a correlation factor better than 0.999 is obtained between the ends of the experimental curve and an extrapolated straight line, but in some cases the correlation could be improved by a quadratic curve. With that procedure, a curve similar to that of Fig. 2 results. That curve only describes the difference in the absorbed heats between sample and reference along points *d* and *c*. The area between that curve and the *x*-axis is precisely the total heat involved in the dissolution process of all the hydride mass.

2.2. $Q_{\delta\to\alpha}$ and TSSd determination

The value of the terminal solubility temperature in dissolution, TSSd, is between T_m and T_c temperatures.

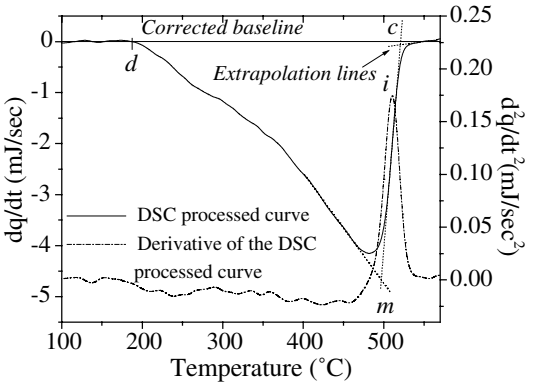

Fig. 2. DSC curve processed subtracting a straight line interpolated between points d and c to the original curve (Fig. 1). Points m, i and c are associated with TSSd.

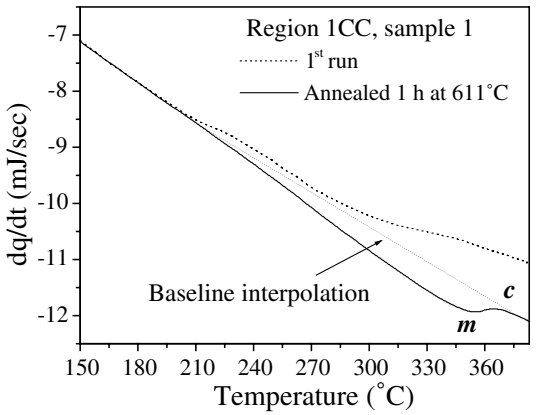

Fig. 3. DSC curves of an irradiated sample. The dotted-line curve corresponds to the first run and the solid-line to a run made after annealing the sample at 600 °C. As can be seen, the baseline is well defined only in the last case.

Based on comparisons with the well-referenced Kearns curve, some authors choose T_m as TSSd [6,7]. On the other hand and based on matters related to the temperature measurement accuracy, other authors choose T_i [5]. From a thermodynamic point of view, the point to be associated to TSSd would be the completion point, c, where the dissolution effects on the DSC curve disappear and the calorimetric curve recovers the base line tendency. The existence of these criteria results in an uncertainty given by the interval (T_m, T_c). Consequently, this work attempted to measure these two temperatures in order to quantify such said uncertainty margin. However, this was only possible with unirradiated material. In the case of irradiated material, in the calorimetric curve corresponding to the first run, irregularities in the base line's recovery – which is the one providing the most useful information – have shown the non-reproducibility of T_c values, precluding its determination. As an example, the DSC curves of the first run and the one obtained after the same sample was annealed at 600 °C is shown in Fig. 3. As can be see, in addition to the small signal of the dissolution process in the first run, the recovery of the baseline is smooth and undefined. As a consequence, for irradiated material, only the dissolution curve (T_m) minimum point $\mathrm{TSSd_{irrad}}$ values have been considered. This information was already presented in a previous work [2].

The dissolution heat, $Q_{\delta\to\alpha}$, is the area enclosed between the calculated $\mathrm{d}\,q(t)/\mathrm{d}\,t$ vs time curve and the x-axis of Fig. 2, and is obtained by numeric integration. Once the sample mass and hydrogen concentration are known, the total hydrogen content (m_{H} in H moles) can be obtained and $\Delta H_{\delta\to\alpha}$ can be determined by the following equation:

$$\Delta H_{\delta\to\alpha} = \frac{Q_{\delta\to\alpha}}{m_{\mathrm{H}}}. \tag{1}$$

3. Original materials

3.1. Unirradiated material

10 cm × 1 cm pieces of material were cut from cold rolled Zircaloy-4 sheets 1.8 mm in thickness. Its chemical composition is given in Table 1. The specimens were recrystallized at 700 °C during 2.5 h. An equiaxed 15–20 μm diameter grain structure was obtained.

3.1.1. Hydriding

The pieces above described were cut in 5 × 1 cm specimens, mechanically polished with SiC paper and then pickled with an aqueous solution of HNO_3 and HF in distilled water. Then, the specimen surfaces were conditioned with an ionic sputtering argon beam and coated with a palladium film. The specimens were charged in a 99.999% pure hydrogen atmosphere at 2.5 kg/mm^2

Table 1
Chemical composition of the unirradiated Zircaloy-4

Alloying elements (wt%)				Impurities (ppm wt%)									
Sn	Fe	Cr	O	Ni	Hf	Al	Co	Cu	Mn	Mo	Ti	U	W
1.49	0.20	0.11	0.14	49	99	39	18	30	36	8	3	1.5	25

and 400 °C during 1/4 to 3 h which produced specimens with different H concentrations covering practically the entire solubility range of the αZr phase.

After charging, all the samples were thermally treated at 450 °C for 3 h in a N_2 atmosphere to homogenize the hydride distribution and then furnace cooled. By X-ray diffraction diagrams (XRD), the equilibrium phase with $ZrH_{1.5}$ to $ZrH_{1.66}$ stoichiometric relations was observed in practically all of them. The metastable γ phase was only observed in two of them. Twenty four $4 \times 4 \times 1.5$ mm samples weighing between 150 and 155 mg and concentrations in the interval 80–640 ppm were obtained for the DSC measurements.

3.1.2. DSC experiments

Prior to the DSC runs, a 1/2 h, 550 °C (eutectoid temperature) solubilization treatment was applied to each sample, to ensure a homogeneous hydride distribution. Experiments were performed under high purity nitrogen (99.998%) 25 ml/min flow at a 20 °C/min heating rate.

The maximum programmed temperature (T_{max}) in each run was 550 °C, with no residence time at T_{max}. Then the cooling was made at the same rate.

To check the reproducibility of the DSC technique and estimate its error, several runs were made on the same sample. For TSSd, the error is slightly lower than 2 °C, and for $Q_{\delta\to\alpha}$, the error is around 6% of the measured value. After measuring the whole series of samples, the hydrogen concentration was measured in each sample with a LECO RH-404 meter.

3.2. Irradiated material

3.2.1. Characterization

The irradiated material was taken from two cooling channels removed from the CNA1 reactor after 10.3 EFPY. One of the channels was situated at the center of the reactor core, CC, and the other in the outer layer of the reactor, OC. These two channels material have a fully recrystallized grain microstructure of about 20 ± 6 μm. Both channels were made of Zircaloy-4 (Table 2).

The cooling channels are made with two concentric welded tubes 6 m long. The inner one, used for the present study, has an OD = 10 cm and is 1.6 mm in thickness. The outer one is a foil of 0.2 mm in thickness. Between them a corrugated foil of 0.1 mm in thickness is inserted to separate the two types of tubes. As the channels are vertically oriented in the reactor core, a temperature rise of about 40 °C exists along the tubes, 263 °C at the inlet and 303 °C at the outlet. After

Table 2
Chemical composition of the irradiated Zircaloy-4 (only the alloying elements)

Channels	Alloying elements (wt%)			
	Sn	Fe	Cr	Ni
Central (CC)	1.6	0.22	0.065	0.0032
Outer (OC)	1.6	0.21	0.07	0.0041

Table 3
Dissolution enthalpies measured in the three initial runs, the stable zone and after the annealings

Reg.	Sample	Fluence ($\times 10^{22}$ n/cm^2)	T_{op} (°C)	[H + D] (ppm-H_{eq})	$\Delta H^{irrad}_{\delta\to\alpha}$ (kJ/mol H)					
					First run	Second run	Third run	Stable zone	After 2 h at	
									508 °C	611 °C
3 OC	2	0.42	280	156	2.5	16.8	20.8	26.8	33.5	–
1CC	1	<0.05	263	179	–	–	–	–	–	34.1
	2			185	–	–	–	–	–	27.4
2 CC	1	0.70	268	157	2.0	9.6	13.7	13.2	12.0	–
	2			159	3.9	8.6	9.4	12.4	12.8	–
	3			174	5.3	9.6	11.1	13.2	13.4	–
3 CC	1	1.00	280	156	7.4	15.3	17.3	20.2	–	25.0
	2			179	11.4	16.7	17.1	21.3	–	24.0
	3			157	6.8	16.2	18.7	18.8	–	23.1
	4			157	5.9	17.3	19.0	18.8	–	23.8
	5			163	–	17.2	17.8	19.5	–	25.0
	6			169	6.5	13.7	15.3	15.2	–	20.8
	7			181	4.5	13.2	13.1	14.0	–	19.4
4 CC	1	0.90	298	211	15.3	23.3	25.1	24.7	29.1	–
	2			260	13.5	18.7	18.7	–	24.4	–
	3			250	11.7	17.3	–	–	29.6	–

Table 4
Dissolution enthalpies measured at the first run and after the annealings

Reg.	Sample	Fluence ($\times 10^{22}$ n/cm^2)	T_{op} (°C)	[H + D] (ppm-H_{eq})	$\Delta H^{irrad}_{\delta\to\alpha}$ (kJ/mol H) first run	T_{rec} (°C)	Annealing time (h)	$\Delta H^{irrad}_{\delta\to\alpha}$ (kJ/mol H)
2 CC	A	0.70	268	178	~3	508	2	16.5
						611	12	23.5
	B			220	1.7	611	83	33.3
3 OC	C	0.42	280	181	3.4	380	32	21.9
						410	32	26.8
						700	1	24.6
	D			381	1.7	380	32	15.7
						611	83	35.4
						700	1	32.5

10.3 years in operation, the fluence reaches a value of about 10^{22} n/cm^2 ($E > 1$ MeV) [8].

The corrosion reaction between the zirconium and the heavy water releases deuterium (D), part of which is incorporated into the metal. In this way, the total equivalent hydrogen isotope concentration in ppm in weight in the metal is given by $[H + D]_{eq} = [H] + 1/2*[D]$, where [H] is the concentration of the original material (about 20 ± 5 ppm). That equivalent concentration increases with the time of residence in the reactor, reaching values as high as 380 ppm-H_{eq}. The [H + D] in the samples was measured with a LECO RH-1 meter. Tables 3 and 4 list the regions from which the samples were removed, the neutron fluence at these regions and the corresponding hydrogen equivalent concentration. The total measurement error of the $[H + D]_{eq}$ is estimated to be 10 ppm in weight.

3.2.2. DSC runs

50–130 mg, rectangular shaped samples were cut from specimens taken from samples of different regions of the channels. Unirradiated Zircaloy-4 samples with 20 ± 5 ppm hydrogen were used as reference. The heating–cooling rate applied to the calorimetric experiments was 20 °C/min, as explained in a previous work [2].

A series of successive triangular thermal cycles, of brief duration, up to $T_{max} = 380$ °C were applied to the first 16-samples. The $TSSd_{irrad}$ and $Q^{irrad}_{\delta\to\alpha}$ values were measured during the heating up of each run. After the whole series were finished, the samples were isothermally annealed at 508 or 611 °C for 2 h. After the annealings, a few cycles up to 380 °C were done again to determine the effects of the annealing.

Another 4-sample batch was isothermally annealed at 611 °C for longer periods of time. The $Q^{irrad}_{\delta\to\alpha}$ was again measured during the heating step of each run. The error in the $Q^{irrad}_{\delta\to\alpha}$ values does not differ from the error estimated for unirradiated material (≅6%), but when irregularities were observed at the first run, the estimated error for $Q^{irrad}_{\delta\to\alpha}$ was increased to 15%. After finishing these series, $[H + D]_{eq}$ was measured in each sample (Tables 3 and 4).

4. Results

4.1. Unirradiated material

4.1.1. TSSd determination

The TSSd value at the minimum (m) and completion (c) points, named $TSSd_1$ and $TSSd_2$, respectively, were determined. A systematic difference of about 30 °C on average was observed between their values independent of hydrogen concentration.

By building the Arrhenius plot, $\ln X$ vs 1/TSSd, the following regressions were obtained:

$$\ln X = 2.59 - 4301/\mathrm{TSSd}_1, \tag{2}$$

$$\ln X = 2.76 - 4582/\mathrm{TSSd}_2, \tag{3}$$

being $X = m_H/m_{Zr}$ the atomic fraction. The strong linearity observed shows that the dissolution enthalpy is independent of temperature along the whole solubility range in the αZr phase. Fig. 4 shows the graphs for Eqs. (2) and (3). The slopes for these straight lines times the ideal gas constant ($R = 8.31 \times 10^{-3}$ kJ/mol K) are 35.6 ± 0.3 kJ/mol H for $TSSd_1$ and 38.1 ± 0.3 kJ/mol H for $TSSd_2$, representing the αZr + δ → αZr transformation enthalpy.

4.1.2. $Q_{\delta\to\alpha}$ direct measurement and $\Delta H_{\delta\to\alpha}$ calculation

The values of $Q_{\delta\to\alpha}$ and $[H + D]_{eq}$ of each Zircaloy-4 sample are drawn in a $Q_{\delta\to\alpha}$ vs m_H (H moles) graph (Fig. 5). From the slope of this linear relation the dissolution enthalpy $\Delta H_{\delta\to\alpha}$ can be determined. The slope value is 39.3 ± 1.2 kJ/mol H, in good agreement with those obtained through the Arrhenius plot for $TSSd_1$ and $TSSd_2$ (see Section 4.1.1). An average value calculated from the Arrhenius values and the $Q_{\delta\to\alpha}$ vs m_H slope is selected for reference proposes; $\Delta H_{\delta\to\alpha} = 37.7$ kJ/mol H.

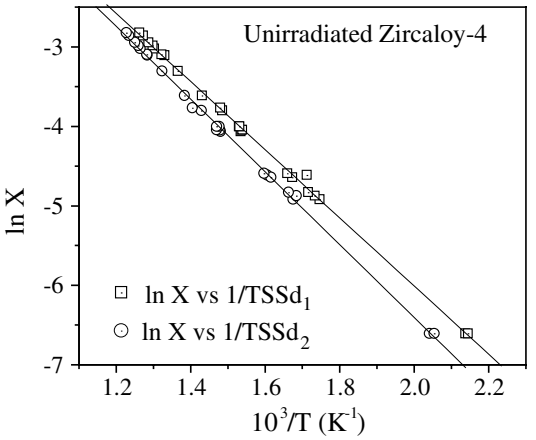

Fig. 4. Due to the high linearity observed in the Arrhenius graphs, the slope of these linear regressions is the solvus or dissolution enthalpy in all the solubility range in αZr phase.

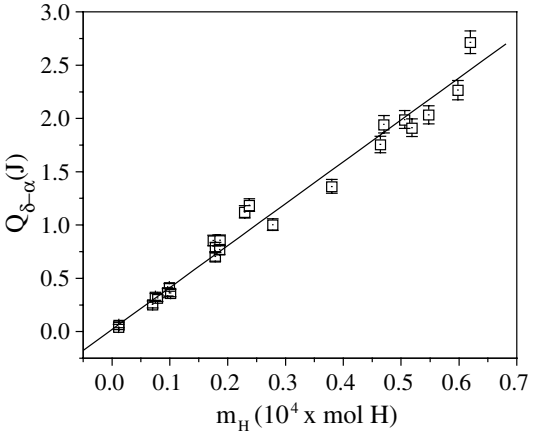

Fig. 5. The relation between $Q_{\delta\to\alpha}$ and m_H ($10^4 \times$ mol H) is highly linear. This implies that the slope of the linear regression is $\Delta H_{\delta\to\alpha}$ in all the solubility range.

4.1.3. $Q^{irrad}_{\delta\to\alpha}$ determination and $\Delta H^{irrad}_{\delta\to\alpha}$ calculation

From Eq. (1), the enthalpy $\Delta H^{irrad}_{\delta\to\alpha}$ was determined for each one of the irradiated samples (Table 3).

$\Delta H^{irrad}_{\delta\to\alpha}$ is observed to change between the first three runs. After the third run the values of $\Delta H^{irrad}_{\delta\to\alpha}$ reaches a stable value. As shown in Table 3, the initial $\Delta H^{irrad}_{\delta\to\alpha}$ values are very low, around 5 kJ/mol H on average, practically an order of magnitude lower than the value measured in unirradiated Zircaloy-4. In addition, the $\Delta H^{irrad}_{\delta\to\alpha}$ values of samples taken from the same region equal $[H + D]_{eq}$ values follow a similar evolution with the number of runs, showing the high reproducibility of the measurement.

The $Q^{irrad}_{\delta\to\alpha}$ values for samples from the Region 1 CC are not reported because the small signal observed in the runs up to 380 °C, and the smoothness of the baseline's recovery at the completion point *c* enlarge the uncertainty in the measurement of the area between the curve and the baseline in the $Q^{irrad}_{\delta\to\alpha}$ determination. However, after annealing at 611 °C the calorimetric experimental curve takes the typical shape and it was possible to calculate $Q^{irrad}_{\delta\to\alpha}$. It should be pointed out that for the Region 1 CC sample 1 reaches the unirradiated material enthalpy value after only 2 h at 611 °C. The pointed behavior can be observed in the Fig. 3.

The resistance to recovery to the unirradiated material $\Delta H_{\delta\to\alpha}$ value seems to increase as the fluence increases and also seems to be a function of irradiation temperature, as observed in the samples coming from the 2 CC, 4 CC and 3 OC regions.

Isothermal treatments at higher annealing temperatures increases the value of $\Delta H^{irrad}_{\delta\to\alpha}$. The $\Delta H^{irrad}_{\delta\to\alpha}$ values of samples from Region 3 CC treated at 611 °C for 2 h are about 25% on average higher than the values in the stable zone, while an increment of only 15% was observed in samples from Region 4 CC treated at 508 °C for 2 h. No significant variations were observed in Region 2 CC after isothermal treatments at 508 °C for 2 h. Thus, in summary, after annealings at 508 °C the $\Delta H^{irrad}_{\delta\to\alpha}$ values are 40% on average lower than the value of unirradiated material, while after annealings at 611 °C are about 30% lower.

Fig. 6 shows the evolution of $\Delta H^{irrad}_{\delta\to\alpha}$ for samples of the region 3 CC with the number of runs and the isothermal treatment. A sharp increase is observed after the first run; the $\Delta H^{irrad}_{\delta\to\alpha}$ value stabilizes after the third or fourth run (stable zone); and after the annealing at 611 °C an additional increment is observed. This figure also shows the high reproducibility of the calorimetric

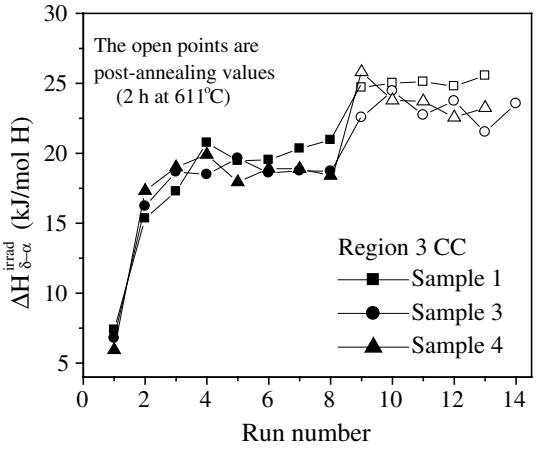

Fig. 6. $\Delta H^{irrad}_{\delta\to\alpha}$ evolution with the successive runs of three samples taken from the Region 3 CC (≅157 ppm-H_{eq}).

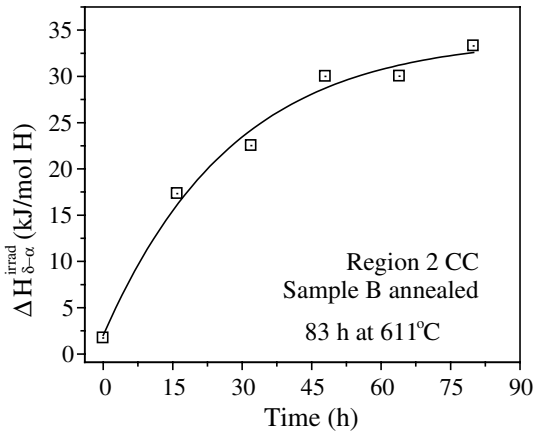

Fig. 7. $\Delta H^{irrad}_{\delta\rightarrow\alpha}$ evolution with long thermal annealings at 611 °C. Sample B of Region 2 CC.

measurements. This is because the shape of the curves corresponding to three samples of identical hydrogen concentration (157 ppm-H_{eq}) are practically equal.

Table 4 shows the results obtained for the samples that were isothermally treated for long periods. For the sample A from Region 2 CC, after 2 h at 508 °C the enthalpy obtained is similar to those of samples subjected to the series of successive runs (Table 3). After the 611 °C treatment has been applied for 12 h, the enthalpy value increases 30%, but still is at least 40% lower than typical values for unirradiated material.

Sample B, also from Region 2 CC, received five subsequent 16-h thermal treatments at 611 °C. The dissolution heat was measured between thermal cycles. Fig. 7 shows the $\Delta H^{irrad}_{\delta\rightarrow\alpha}$ evolution after each treatment. The final value, after 83 h at 611 °C, is 33.5 kJ/mol H, which is within the literature range of values for the δ hydride dissolution enthalpy in unirradiated Zircaloy-4.

Sample C (Region 3 OC) was isothermally treated at 380 °C during 32 h followed by a final treatment of 32-h at 410 °C. That treatment was applied to check the stability of the $\Delta H^{irrad}_{\delta\rightarrow\alpha}$ in the stable zone that were observed in the series of runs made up to T_{max} 380 °C (Table 3). The values obtained after 32 h at 380 °C differs by only 10% of the value after 32 h at 410 °C. Considering the experimental error, both values are considered equal. They are still 35% lower than the value corresponding to unirradiated material.

Finally, in Sample D (Region 3 OC) a series of consecutive annealings at 380 °C, totaling 32 h was applied. The development of a wide stable zone is again verified. Furthermore after a series of annealings at 611 °C, accumulating 83 h $\Delta H^{irrad}_{\delta\rightarrow\alpha}$ reaches a value of $\Delta H^{irrad}_{\delta\rightarrow\alpha} =$ 35.3 kJ/mol H, which is practically equal to that of unirradiated material (Fig. 8).

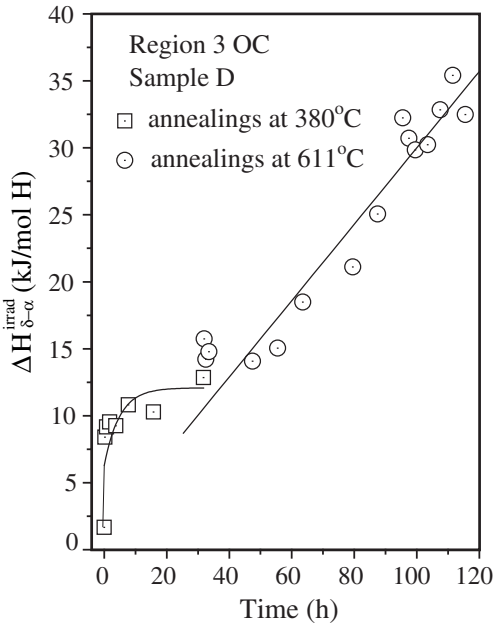

Fig. 8. $\Delta H^{irrad}_{\delta\rightarrow\alpha}$ evolution with long thermal annealings at 380 and 611 °C in sample D, Region 3 OC.

5. Discussion

5.1. Unirradiated material

5.1.1. αZr/[αZr + δ] solvus line

The αZr/[αZr + δ] phase limits obtained according to the minimum ($TSSd_1$) and completion ($TSSd_2$) criteria have been compared to curves obtained from the measurements by Zuzek and Kearns [3,5]. By converting Eqs. (2) and (3), the following expressions are obtained:

$$X_1\{\alpha Zr/[\alpha Zr + \delta]\} = 13.28\exp(-4301/TSSd_1), \quad (4)$$

$$X_2\{\alpha Zr/[\alpha Zr + \delta]\} = 15.77\exp(-4582/TSSd_2), \quad (5)$$

where X = H/Zr (atomic fraction) and $TSSd_{1;2}$ are in Kelvin.

Fig. 9 shows these curves as well as those by Zuzek and Kearns. Zuzek's solvus line corresponds to data selected from the literature by the author, obtained through equilibrium, calorimetric and dilatometric methods [3]. This curve agrees very well with the one adjusted in this work based on the $TSSd_2$ (curve C_2) values throughout the concentration range. The same applies to the solubility curve in Kearns's work, which is one of the most referenced solubility curves in the literature. On the other hand the curve obtained from $TSSd_1$ values (curve C1, Eq. (4)) falls down in the high concentration region of the αZr phase solubility interval. An extended discussion about this topics was given in [1,9].

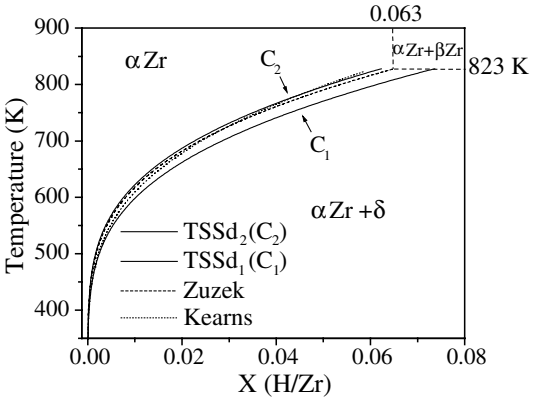

Fig. 9. Curves C_1 and C_2 fitted using $TSSd_1$ and $TSSd_2$ data in the present work compared with Kearns and Zuzek curves.

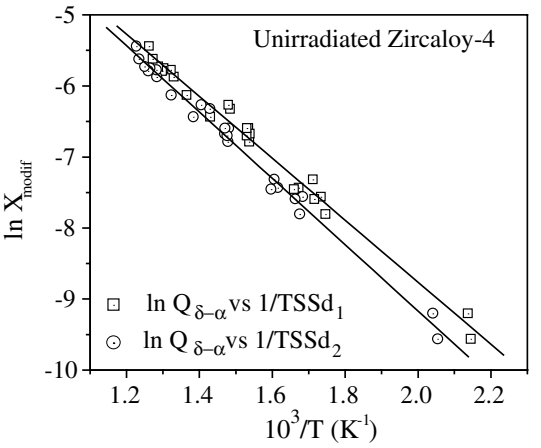

Fig. 10. Arrhenius graph modified using the $Q_{\delta\to\alpha}$ direct measurements for unirradiated Zircaloy-4 data.

Table 5
Comparison between the $\Delta H_{\delta\to\alpha}$ literature data and the present work data (unirradiated Zircaloy-4)

Reference	$\Delta H_{\delta\to\alpha}$ (kJ/mol H)
Present work (Arrhenius)	37.6 ± 0.9
Present work (direct method)	39.3 ± 1.2
Zuzek	37.9
Dantzer	37.7

5.1.2. αZr + δ → αZr transformation enthalpy

Two different procedures were used to calculate $\Delta H_{\delta\to\alpha}$, one based on the measurements of TSSd (Arrhenius graphs) and the other based on the $Q_{\delta\to\alpha}$ values (Eq. (1)). In both, the $\Delta H_{\delta\to\alpha}$ is given by the slope of a linear regression. The values given by the Arrhenius graphs (Fig. 4) and the $Q_{\delta\to\alpha}$ vs m_H relation (Fig. 5) together with those given by Zuzek and Dantzer [3,4], are shown in Table 5. All values proved to be very consistent with each other, so that both procedures can be applied to obtain the αZr + δ → αZr enthalpy.

Besides showing the accuracy and self consistency of the DSC technique, the above-mentioned results show the proportionality between $Q_{\delta\to\alpha}$ and $m_{H.}$ With that proportionality it is not necessary to know the hydrogen concentration to calculate the enthalpy. Replacing in the Arrhenius law:

$$\ln X = \frac{\Delta S_{\delta\to\alpha}}{R} + \frac{\Delta H_{\delta\to\alpha}}{RT}, \tag{6}$$

where R is the ideal gas constant, $\Delta S_{\delta\to\alpha}$ is the dissolution entropy and $\Delta H_{\delta\to\alpha}$ is the enthalpy. If Eq. (6) is combined with Eq. (1), we obtain:

$$\ln X_{\text{modif}} = \frac{\Delta S_{\delta\to\alpha}}{R} + \frac{\Delta H_{\delta\to\alpha}}{RT}, \tag{7}$$

where we define $X_{\text{modif}} = Q_{\delta\to\alpha}/m_{Zr}\Delta H^{(A)}_{\delta\to\alpha}$, considering $\Delta H^{(A)}_{\delta\to\alpha}$ as $Q_{\delta\to\alpha}$ normalization factor which, for simplicity reasons, we will choose to be 36.9 kJ/mol H (the average value obtained through Arrhenius in 4.1.1). Fig. 10 shows the linear regressions in $\ln X_{\text{modif}}$ vs $1/TSSd_{1;2}$.

The slopes are 36.3 ± 0.9 kJ/mol H for $TSSd_1$ and 38.8 ± 0.8 kJ/mol H for $TSSd_2$ (37.6 ± 1.6 kJ/mol H in average), in accordance with the values obtained in this work and in those presented in the literature. This relation will be useful to understand the results obtained in irradiated material.

5.2. Irradiated material

The low $\Delta H^{\text{irrad}}_{\delta\to\alpha}$ values obtained in the first calorimetric run and their increase with the subsequent annealings to which the samples were subjected are in agreement with the evolution observed in $TSSd_{\text{irrad}}$ in this material in a previous work [2]. A decrease in the solubility temperature, i.e., an increase in hydrogen solubility, must be accompanied by a decrease in the dissolution enthalpy, since it controls the dissolution process.

According to the results observed in Table 3, the hydride dissolution enthalpy in an irradiated αZr matrix is inferred to be much lower than that of the δ phase in unirradiated Zircaloy-4. In addition, said enthalpy increases with annealings and tends to the unirradiated δ phase value. Three stages are observed in the $\Delta H^{\text{irrad}}_{\delta\to\alpha}$ evolution to the unirradiated value:

1. A first stage, consisting of the values obtained during the first three runs up to 380 °C, where the enthalpy grows very fast with the number of runs.
2. A second stage where the enthalpy is constant along the successive runs even when the holding time at $T_{\max}$ extends for several hours.
3. A third stage, characterized by a monotonic growth of the enthalpy value with the isothermal time at 508 °C and 611 °C, until an equilibrium value is reached.

The low value of $\Delta H_{\delta\to\alpha}$ in irradiated material might be attributed in principle to the precipitation of a new type of intermediate hydride phase. This hypothesis is based on the great number of irradiation induced crystalline defects in the irradiated material that could act as nucleation sites. However, XRD measurements made in irradiated Zircaloy-4 taken from fuel claddings show the presence in the diffraction pattern of peaks from the δ and γ hydride phases only [10]. On the other hand, the $\Delta H^{\text{irrad}}_{\delta\to\alpha}$ values that were measured in the present work after the first few runs (Tables 3 and 4) are an order of magnitude lower than the δ phase dissolution enthalpy, 37.7 kJ/mol H in Zr and other hydride-forming metals [11,12].

The presence of γ phase could possibly explain the observed phenomenon. Some authors have argued that it is a stable phase forming at low hydrogen concentrations, which completely transforms to δ at 255 °C [13]. Both, the precipitation manner and the alleged stability of γ phase aroused theoretical interest during the '70 s. Although some later experimental and theoretical works are more in favor of a γ phase metastability, the topic is still under discussion [3,14].

The $\Delta H^{\text{irrad}}_{\delta\to\alpha}$ values obtained in the first and second calorimetric runs (columns 6 and 7, Table 3) are quite close to the 10 kJ/mol H value obtained by Mishra et al. in the low concentration region ([H] < 60 ppm), which the author assigns to the γ phase dissolution enthalpy [15]. Based on the information found in the literature, the precipitation of γ phase appears to be associated with a hydrogen supersaturation phenomenon in solid solution when the cooling rates are high (quenching). This phenomenon has been observed for low and intermediate concentrations (200 ppm) but is favored in low concentration regions [16,17].

Although the presence of γ phase in fuel claddings removed from reactors was observed [10], is difficult to explain this phenomena in terms of high cooling rates because final cooling rate in-reactor is not a quenching rate. Turning to the analysis of the data obtained in this work and analyzing the presence of γ phase under the scope of cooling rates, even if all the hydride present in the irradiated samples 'as received' were and its contribution to the enthalpy according to the equation:

$$\Delta H = f_\delta \Delta H_{\delta\to\alpha} + f_\gamma \Delta H_{\gamma\to\alpha} \tag{8}$$

were close to 100% ($f_\delta \to 0$), this contribution should change dramatically after the first calorimetric run, since the cooling is done at 20 °C/min, which is closer to typical/furnace cooling rates (5 °C/min) than quenching rates (≈600 °C/min). Therefore, enthalpy values close to the δ equilibrium phase should be obtained in the second run, but this has not been observed. In addition, there should not be subsequent increases in $\Delta H^{\text{irrad}}_{\delta\to\alpha}$ after the second run or after the 2-h or longer annealings, since the cooling was made at the same rate in all the cases, but this has in fact been observed. Thus, if the low enthalpy values of irradiated material were caused by the presence of the γ phase, no enthalpy values dramatically different from those of unirradiated material should be obtained after the first run and the subsequent annealings. Then, the overall behavior observed in irradiated material cannot be explained by this hypothesis.

On the other hand, as was previously discussed by Mc Minn et al. in [5], a relation between hydride precipitation and the irradiation hardening can be considered. The strengthening caused by the neutron irradiation could make favorable the dissolution of the hydrides. Due to the difference in specific volume between the matrix and hydrides the dissolution process should be facilitated, having a relaxation effect on the strengthened matrix. Furthermore, this strengthened condition of the matrix makes less favorable the onset of the precipitation process [5]. To evaluate the application of that hypothesis should be taken into account that all the samples studied in the present work have $[H + D]_{eq}$ values higher than 150 ppm-H_{eq}. Then, in an unirradiated matrix with a bulk [H] of 200 ppm for example, about 130–160 ppm of hydrogen are precipitated as hydrides at the operation temperature range (260–300 °C) and the rest is in solid solution. In the present case, the bulk $[H + D]_{eq}$ was built up by the incorporation of deuterium atoms at a rate defined by the corrosion reaction, which, assuming a linear law, will be of about 15–20 ppm-H_{eq} per year. If some mechanical stress was built up due to the difference in specific volume between an irradiated matrix and the zirconium hydrides, it will be enough time at the operation temperature to allow the relaxation of the mechanical stresses by some kind of creep mechanism. Then, only the hydrogen/deuterium atoms in solid solution at the operation temperature could develop mechanical stresses between them and the irradiation strengthened matrix during the shut down of the reactor. There is no reason to assume that this small fraction of the hydrogen/deuterium bulk content (40–70 ppm-H_{eq}) precipitated in the pointed conditions could be dissolved at lower temperature and affect the dissolution process to reduce the TSSd value in 100 °C. In addition, that hypothesis could not explain the evolution of $TSSd_{irrad}$ with the number of runs and isothermal annealings at high temperatures as 600 °C.

However, the low $\Delta H^{\text{irrad}}_{\delta\to\alpha}$ values in the first run, and the subsequent incremental increases in $\Delta H^{\text{irrad}}_{\delta\to\alpha}$ with annealings are compatible with the *hydrogen trapping hypothesis* presented in previous works [2,5,18]. As is well known the hydrogen isotope concentration increases with the time in operation because a fraction of the total amount of deuterium that is released during the corrosion reaction of the zirconium with the aqueous media will be incorporated into the material. Then, according to this hypothesis when the concentration

limit is exceeded, the fraction of the hydrogen isotopes in excess will be trapped by crystalline defects generated by irradiation, instead of precipitating as hydrides [2]. The decreased enthalpy seen in irradiated material would be due to the fact that the actual amount of hydrogen precipitated as hydrides is much lower than the bulk hydrogen concentration. In consequence the enthalpy values calculated from Eq. (1) lead to $\Delta H^{\text{irrad}}_{\delta\to\alpha}$ values lower than $\Delta H_{\delta\to\alpha}$.

The value estimated by Lewis for the defect-hydrogen interaction enthalpy in Zr is 26.8 kJ/mol H (0.28 eV/atom) [18], which is lower than the $\Delta H_{\delta\to\alpha}$ values obtained for unirradiated material in this work and also lower than the precipitation values which may be found in the literature, such as the 32.5 kJ/mol H measured by Erikson [19]. In consequence, the defects are energetically favorable sites for hydrogen atoms competing with the hydride precipitation.

The $\Delta H_{\delta\to\alpha}$ determination, made both through the Arrhenius correlation and directly by means of Eq. (1) provides additional support to the *hydrogen trap* hypothesis through Eq. (7). Given the proportionality relation between $Q_{\delta\to\alpha}$ and the hydrogen content, this equation allows us to obtain the dissolution enthalpy without measuring the hydrogen concentration. The evolution of $Q^{\text{irrad}}_{\delta\to\alpha}$ and $\text{TSSd}_{\text{irrad}}$ with annealings observed in irradiated samples allows us to build the $\ln X_{\text{eff}}$ vs $1/\text{TSSd}_{\text{irrad}}$ graph with data corresponding to only one irradiated sample, where:

$$X_{\text{eff}} = \frac{m_{\text{H}_{\text{eff}}}}{m_{\text{Zr}}}. \tag{9}$$

In Eq. (9) we define $m_{\text{H}_{\text{eff}}} = Q^{\text{irrad}}_{\delta\to\alpha}/\Delta H^{(\text{ref})}_{\delta\to\alpha}$ as the hydrogen content (in moles) which is actually precipitated as hydrides in the irradiated sample at room temperature, m_{Zr} is the sample mass (in moles of Zr) while $\Delta H^{(\text{ref})}_{\delta\to\alpha}$ is the enthalpy value of unirradiated Zircaloy-4 taken as reference, 37.6 kJ/mol H, an average value obtained from the regressions in Fig. 10.

If no one 'unstable' zirconium hydride phase than the equilibrium δ-hydride precipitates in the irradiated material, the enthalpy value arising from the slope in these graphs should not differ essentially from that obtained for unirradiated Zircaloy-4, or in more accurate terms, from the values obtained from linear regressions in Fig. 10, between 36.3 ± 0.9 kJ/mol H and 38.8 ± 0.8 kJ/mol H.

There is no doubt that the most appropriate samples to build a graph of this type are those which were subjected to long annealings at 611 °C, especially samples B from Region 2CC and D from Region 3 OC which, during their recovery, cover a solubility temperature range equivalent to a range of concentrations of 130 and 200 ppm-$H_{eq,}$ respectively. In order to build this graph, the $Q^{\text{irrad}}_{\delta\to\alpha}$ values measured in this work in the samples B and D after long annealing times (from which

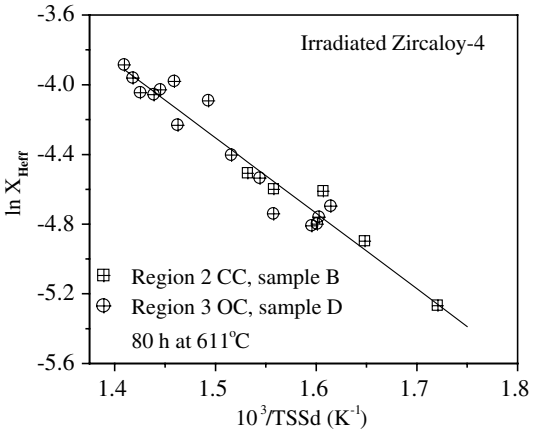

Fig. 11. Modified Arrhenius graph built with the data of the samples B and D of the Regions 2 CC and 3 OC respectively.

$\Delta H^{\text{irrad}}_{\delta\to\alpha}$ was calculated by Eq. (1) and plotted in the $\Delta H^{\text{irrad}}_{\delta\to\alpha}$ vs annealing time curves in the Figs. 7 and 8) and the $\text{TSSd}_{\text{irrad}}$ values corresponding to the same samples already presented in a previous work [2], were used. Fig. 11 shows the experimental values and the linear regression, the correlation coefficient is 0.97, which shows an acceptable linearity, and the enthalpy value obtained is 36.0 ± 2.1 kJ/mol H, which perfectly agrees with the values measured in unirradiated material, showing that only an effective hydride mass smaller than the total bulk hydrogen concentration is dissolved in the irradiated sample after each successive thermal treatment which increases the effective hydride mass. This behavior is compatible with the hydrogen trapping hypothesis.

6. Conclusions

The enthalpy values obtained in the first calorimetric run for irradiated Zircaloy-4 are around 5 kJ/mol H in average, well below the values of unirradiated material. These initial values are not stable; they increase with the annealings implicit in the subsequent calorimetric runs until a stable zone is reached, where the $\Delta H^{\text{irrad}}_{\delta\to\alpha}$ values are up to 50% of those of unirradiated material. These values increase slightly with 500 °C annealings, and to a greater extent with 600 °C annealings. However, they recover to the values of unirradiated material only slowly with long 600 °C annealings. This behavior is compatible with that observed in previous works in the terminal solubility temperature and supports the idea of the existence of a hydrogen trapping mechanism in defects created by irradiation. The defects are annihilated with the annealings, setting the hydrogen trapped in them free. In this way, the hydrogen fraction

previously trapped in defects is 'available' to precipitate as hydrides when the material is cooled down, increasing the $TSSd_{irrad}$ and $\Delta H^{irrad}_{\delta\rightarrow\alpha}$ in a subsequent run. This model explains the evolution of the dissolution enthalpy.

References

[1] P. Vizcaíno, PhD thesis, Number TD-11/03, Inst. Tech. 'Prof. Jorge A. Sábato', CICAC, CNEA, Buenos Aires, Argentina, 24 June 2003.
[2] P. Vizcaíno, A.D. Banchik, J.P. Abriata, J. Nucl. Mater. 304/2–3 (2002) 96.
[3] E. Zuzek, J.P. Abriata, A. San Martín, F.D. Manchester, Bull. Alloy Phase Diag. 11 (4) (1990) 385.
[4] P. Dantzer, W. Luo, T.B. Flanagan, J.D. Clewley, Metall. Trans. A 24A (1993) 1471.
[5] A. McMinn, E.C. Darby, J.S. Schofield, Zirconium in the Nuclear Industry: Twelfth International Symposium, ASTM STP 1354, 2000, p. 173.
[6] J.J. Kearns, J. Nucl. Mater. 22 (1967) 292.
[7] D. Khatamian, V.C. Ling, J. Alloys Compd. 253&254 (1997) 162.
[8] C. Grant, PUMA System, Version 4 for Windows, Argentine Nuclear Atomic Energy, Avenida Del Libertador 8250, Buenos Aires, Argentina, Technical Internal Report, CNEA.C.RCN.MUS- 034, 1999.
[9] P. Vizcaíno, A.D. Banchik, J.P. Abriata, Metall. Mater. Trans. A 35A (8) (2004) 2343.
[10] M.R. Warren, D.K. Bhattacharya, J. Nucl. Mater. 56 (1975) 121.
[11] W. Luo, T.B. Flanagan, J.D. Clewley, P. Dantzer, Metall. Trans. A 24A (1993) 2623.
[12] Y. Fukai, The Metal-Hydrogen System, Basic Bulk Properties, Springer Series in Materials Science, Springer-Verlag, Berlin, Heidelberg, New York, 1993.
[13] S. Mishra, K.S. Sivaramakrishnan, M.K. Asundi, J. Nucl. Mater. 45 (1972/1973) 235.
[14] K. Une, S. Ishimoto, J. Nucl. Mater. 322 (2003) 66.
[15] S. Mishra, M.K. Asundi, ASTM STP 551, American Society for Testing and Materials (1974) 63.
[16] B. Nath, G.W. Lorimer, N. Ridley, J. Nucl. Mater. 49 (1973/1974) 262.
[17] B. Nath, G.W. Lorimer, N. Ridley, J. Nucl. Mater. 58 (1975) 153.
[18] M.B. Lewis, J. Nucl. Mater. 125 (1984) 152.
[19] W.H. Erickson, D. Hardie, J. Nucl. Mater. 13 (1964) 254.